Solar Energy 135 (2016) 590–597

Contents lists available at ScienceDirect

Solar Energy

journal homepage: www.elsevier.com/locate/solener

An in-depth analysis of the modelling of organic solar cells using multiple-diode circuits

Fernando De Castro [a], Antonino Laudani [b,*], Francesco Riganti Fulginei [b], Alessandro Salvini [b]

[a] National Physical Laboratory, Hampton Rd, Teddington, UK
[b] Department of Engineering, Roma Tre University, V. Vito Volterra, 62, Roma I-00146, Italy

ARTICLE INFO

Article history:
Received 20 April 2016
Received in revised form 11 June 2016
Accepted 13 June 2016
Available online 20 June 2016

Keywords:
Organic solar cells
PV modelling
I–V curve
Circuital model

ABSTRACT

In this paper, an in-depth analysis of the current–voltage characteristics of organic solar cells is performed by introducing a new one-equation model based on a generalised equivalent circuit capable of accurately fitting ideal and non-ideal curves. The model is based on the introduction of a non-linear series resistance term that can be reduced to a linear resistance for the case of ideal curves. A hybrid optimiser approach is proposed combining genetic algorithms and deterministic methods that is shown to facilitate the extraction of the parameters and to accelerate the analysis of the identification problem. Our model is compared with state-of-the-art circuits found in the literature and validated though successful fitting of several experimental curves with differing levels of non-ideal behaviour (such as kinks and s-shape).

1. Introduction

Organic solar cells (Organic PhotoVoltaic – OPV) are approaching commercial viability with reported power conversion efficiency of over 13% and encouraging lifetimes (Green et al., 2016; Kong et al., 2014; Heliatek, 2016). Different from crystalline silicon (c-Si) cells, OPVs are not a single technology as manufacturers and research labs use different active layer materials (e.g. organic semiconductor, interlayers, etc.) and various device architectures. That poses challenges to development of the area. One way to accelerate the optimisation and identification of issues during R&D and upscaling is through the development of a list of parameters that can be extracted from simple characterisation tools and correlated/attributed to physical processes in the device. A common procedure in standard solar cells is the parametrisation of current–voltage curves. Fig. 1(a) shows the typical single-diode equivalent circuit used to describe the ideal electric behaviour of c-Si cells. For solar cells that do not behave ideally, this model is no longer valid and many authors have proposed modifications to fit experimental data. In particular in copper–indium–gallium–selenide (CIGS) solar cells and organic solar cells, sometimes a kink (that we will refer to as s-shape) is observed in the current voltage curves (Wagenpfahl et al., 2010) that cannot be modelled by the circuit in Fig. 1(a) (Romero et al., 2012). For a complete discussion on this s-shape *I–V* characteristic we remand to the works of Wagenpfahl et al. (2010) and Sandberg et al. (2014) and to the references within. Amongst the first proposed equivalent circuits, modifications were presented to the single-diode model for OPV as lumped parameters equivalent circuits, by substituting single diode with multiple diodes in parallel (Cheknane et al., 2008), or with complex not linear resistor blocks consisting of ideal diodes, a real diode and variable resistors (Mazhari, 2006). Unfortunately these solutions were again not suitable to simulate effectively s-shape behaviour. The circuit model that can simulate that behaviour was proposed by one of the authors (de Castro et al., 2010) (Fig. 1(b)) and later expanded by other groups (del Pozo et al., 2012; Romero et al., 2012; Garcia-Sanchez et al., 2013). It includes a second diode shunted by a resistor to simulate a region of the device (normally one of the interfaces) where charge accumulation leads to a change in the local electric field and as a consequence generates a charge injection process that is voltage dependent. When the current through the reverse second diode is small (good interface) the circuit of Fig. 1(b) reverts to that in Fig. 1(a). Although that reverse second-diode model could fit experimental data well within a limited voltage range, it relied on approximations to reduce the computational time and it did not include a term that would allow the current to increase again in forward bias after the s-shape. Recently Garcia-Sanchez et al. proposed an extension of that model replacing the resistance that shunts the reverse 2-diode by a third diode (Fig. 1(c)). The authors only solved the resulting equation for a few very specific cases where an explicit solution could be found. In those cases they could fit the full range of experimental current–voltage curve with s-shape. Clearly the

* Corresponding author.
E-mail addresses: fernando.castro@npl.co.uk (F. De Castro), alaudani@uniroma3.it (A. Laudani), riganti@uniroma3.it (F. Riganti Fulginei), asalvini@uniroma3.it (A. Salvini).

http://dx.doi.org/10.1016/j.solener.2016.06.033
0038-092X/

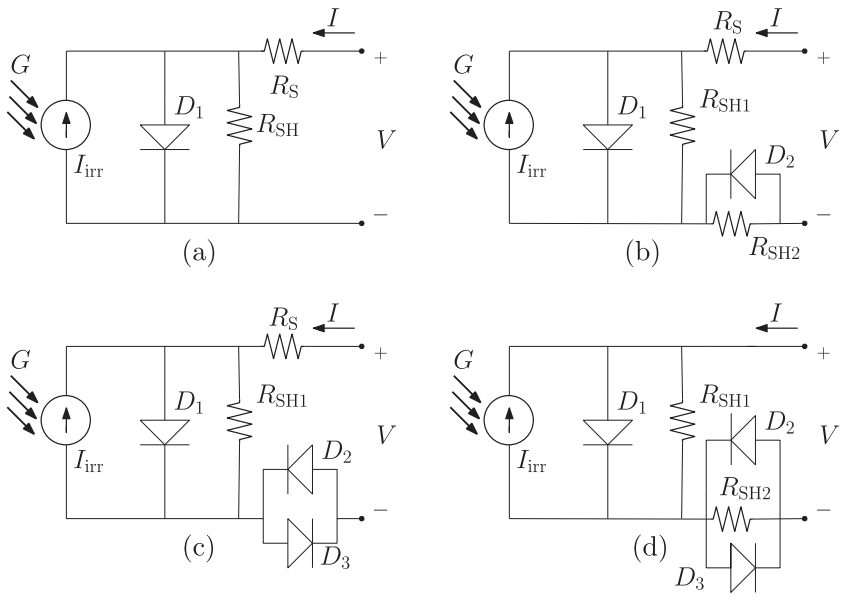

Fig. 1. One and multi diode equivalent circuit models for organic PV. (a) Traditional 1-diode model used for Si solar cells, (b) reverse 2-diode model (de Castro et al., 2010), (c) 3-diode model proposed by Garcia-Sanchez et al. (2013) that expands reverse 2-diode model to fit larger voltage range, and (d) new, generalised 3-diode model proposed in this paper.

validation and the choice of a model in favour of another is also linked to the possibility of finding physical parameters that are able to represent experimental data. This should be the solution of a well-posed identification problem. Unfortunately, for solar cells, one of the difficulties with fitting experimental data with equivalent circuits is that equations are transcendental and often the solution requires approximations. Iterations are also computationally expensive, which makes the procedure impractical when the number of curves to be analysed becomes very large. Therefore many authors rely on implications and approximations (Laudani et al., 2014; de Castro et al., 2010). A breakthrough was achieved in 2000 with the realisation that the Lambert W-function (Corless et al., 1996) could be used to provide an exact analytical solution to the current voltage curve of a diode with series resistance (Banwell and Jayakumar, 2000) and of a diode with both series and shunt resistance (Ortiz-Conde et al., 2000). Then, several authors have exploited the Lambert W-function to solve the current–voltage fitting problem for inorganic (Laudani et al., 2014; Jain and Kapoor, 2004) and organic photovoltaic devices (Jain and Kapoor, 2005; Romero et al., 2012). A few years ago Romero et al. proposed a solution for the reverse 2-diode model in Fig. 1(b). The solution found is very important since it expresses the relation *V*–*I* with a one-equation formula, but it has an important drawback due to the fact that it expresses voltage (*V*) as a function of current (*I*), whereas the measurements are usually done by setting the voltage and measuring the current. On the other hand, one of the main problems to be overcome when one tries to identify a model is to find the most suitable expression describing the model itself. Also in the case of organic solar cells this represents a significant issue which has led several authors in literature to use approximate formulas (de Castro et al., 2010) or complicated expressions based on circuital considerations (del Pozo et al., 2012).

This does not only influence the performance of the fitting routines, but also makes their accuracy difficult to evaluate. For this reason, in this work we present an improved methodology exploiting the use of exact one-equation formulas, different from what is available in the literature. We exploit the reverse 2-diode model and we propose a new, generalised 3-diode model (shown in Fig. 1(d)), to gain insight into the modelling and parametrisation of organic solar cell current voltage curves.

The paper is structured as follows: in Section 2 a short description of the used experimental data is reported; in Section 3 the one-equation model for 2-diode circuit (Fig. 1(b)) is presented, with a discussion on the limitations of the use of this model for the description of the current–voltage curves; in Section 4 the proposed 3-diode model is discussed and its advantages in the modelling OPV are demonstrated and validated by fitting a series of experimental organic solar cell curves with different degrees of s-shape; authors' conclusions follow in Section 5.

2. Measurements and experimental data

The solar cell devices were an enhanced bilayer of purified Poly [2-methoxy-5-(2-ethylhexyloxy)-1,4-phenylene-vinylene] (MEH-PPV, M_n = 40,000–70,000, Aldrich) acting as electron donor and fullerene C60 (>99.95%, SES Research) acting as electron acceptor. Films were fabricated on cleaned (Castro et al., 2006; de Castro et al., 2010) ITO-coated glass coated with 50 nm of PEDOT:PSS (Aldrich, conductivity 1 S cm^{-1}) and subsequently coated with 50 nm of Al to serve as the cathode. Sample fabrication and characterisation was performed in inert N_2 atmosphere. Details of device sample preparation and characterisation were reported previously (Castro et al., 2006; de Castro et al., 2010). Current voltage curves were measured under inert N_2 atmosphere with samples exposed to 1000 W/m^2 simulated AM1.5G sunlight. Thermal annealing at different temperatures was used to reduce the s-shape as previously described (see Fig. 2 de Castro et al., 2010). In this manuscript we fitted curves of devices not annealed and annealed for 5 min at 120 °C, 150 °C, 180 °C and 200 °C. We refer to these samples as naIV100, a120C5min100, a150C5min100, a180C5min100 and a200C5min100, respectively. The experimental *I*—*V* curves for these data are shown in Fig. 2. It is possible to note that the samples, as prepared, show strong s-shapes.

3. The one-equation model for the two-diode circuital representation of an OPV

In this paragraph we describe how to obtain the one-equation model representing the mathematical relation between voltage *V*

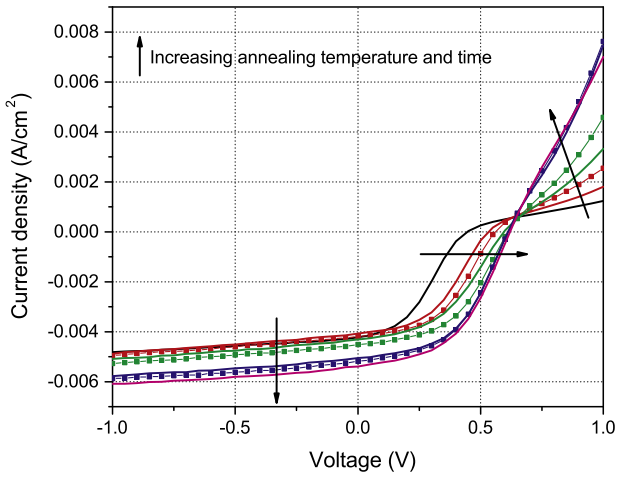

Fig. 2. Experimental organic solar cell current–voltage curves with differing degrees of non-ideal behaviour, from strong s-shape to almost ideal diode-behaviour. Black line represents curve of as prepared (not annealed sample). Arrows indicate direction of change when samples are annealed at different temperatures (120 °C (red lines), 150 °C (blue lines), 180 °C (green lines), 200 °C (magenta line)) and increasing annealing time (5 min (thick line), 15 min (thin line + square symbol)). Such curves cannot be fitted using the traditional model in Fig. 1 (a). (For interpretation of the references to colour in this figure legend, the reader is referred to the web version of this article.)

and current I at the output of the reverse 2-diode circuit (del Pozo et al., 2012; Romero et al., 2012; Garcia-Sanchez et al., 2013). The most adopted traditional model of organic solar cells utilises two diodes as shown in Fig. 1(b) (de Castro et al., 2010; Romero et al., 2014). Let's call V_{D1} and V_{D2} the direct voltages of the two diodes D_1 and D_2, respectively, and let's write the following Kirchhoff's voltage law (KVL):

$$V = R_S I + V_{D1} - V_{D2} \tag{1}$$

Now it is possible to express the voltages V_{D1}, V_{D2} as functions of the currents crossing their branches by using the Lambert W function Corless et al. (1996):

$$V_{D1} = (I + I_{irr} + I_{01})R_{SH1} - n_1 V_T W\left(\frac{I_{01}R_{SH1}}{n_1 V_T} e^{\frac{(I+I_{irr}+I_{01})R_{SH1}}{n_1 V_T}}\right) \tag{2}$$

$$V_{D2} = (-I + I_{02})R_{SH2} - n_2 V_T W\left(\frac{I_{02}R_{SH2}}{n_2 V_T} e^{\frac{(-I+I_{02})R_{SH2}}{n_2 V_T}}\right) \tag{3}$$

where I_{01} and I_{02} are the saturation currents and n_1 and n_2 are the ideality factors of diodes D_1 and D_2, respectively, I_{irr} is the photo-generated current and $V_T = K_B T/q$ is the thermal voltage (where k_B is the Boltzmann constant, T is the temperature and q is the elementary charge). Using Eqs. (2) and (3), the Eq. (1) becomes:

$$\begin{aligned} V = {} & R_S I + (I + I_{irr} + I_{01})R_{SH1} - n_1 V_T W\left(\frac{I_{01}R_{SH1}}{n_1 V_T} e^{\frac{(I+I_{irr}+I_{01})R_{SH1}}{n_1 V_T}}\right) \\ & - (-I + I_{02})R_{SH2} + n_2 V_T W\left(\frac{I_{02}R_{SH2}}{n_2 V_T} e^{\frac{(-I+I_{02})R_{SH2}}{n_2 V_T}}\right) \end{aligned} \tag{4}$$

that can be also reorganized as follows:

$$\begin{aligned} V = {} & I(R_S + R_{SH1} + R_{SH2}) + (I_{irr} + I_{01})R_{SH1} - I_{02}R_{SH2} \\ & - n_1 V_T W\left(\frac{I_{01}R_{SH1}}{n_1 V_T} e^{\frac{(I+I_{irr}+I_{01})R_{SH1}}{n_1 V_T}}\right) \\ & + n_2 V_T W\left(\frac{I_{02}R_{SH2}}{n_2 V_T} e^{\frac{(-I+I_{02})R_{SH2}}{n_2 V_T}}\right) \end{aligned} \tag{5}$$

The expression (5) is important since it expresses the voltage–current relationship using a single equation. Unfortunately, the fact that V is expressed as a function of I leads to a bad formulation of the nonlinear least square problem used for the identification of the parameters, and influences the results. Indeed, since the measurements are usually done by setting the voltage and measuring the current (i.e., we assume a correct value for voltage, whilst the value of current is subject to measurement errors), the independent variable for the definition of the non-linear least square problem should be the voltage and not the current as in the case of using Eq. (5). For this reason, we tried to develop an alternative equation. Indeed, it is possible to further exploit the Lambert W function in order to achieve a new exact one-equation expression, where the current I can be computed from V. This is beneficial as it provides an accurate mathematical expression which can be implemented for fitting without requiring the use of circuital solver or tailored environment, such as Matlab and Mathematica. Indeed, such kind of expression can be directly used for implementation of a least squares algorithm in C or Fortran languages, which can assure a more direct control of the identification procedure. The novel one-equation formula is obtained as follows. First, the current I can be expressed as:

$$I = V_{D1}/R_{SH1} + I_{01}\left[e^{\frac{V_{D1}}{n_1 V_T}} - 1\right] - I_{irr} \tag{6}$$

or also as:

$$I = -V_{D2}/R_{SH2} - I_{02}\left[e^{\frac{V_{D2}}{n_2 V_T}} - 1\right] \tag{7}$$

By considering the Eq. (3) and the expression $V_{D1} = V + V_{D2} - R_S I$, obtained from Eq. (1), we can write:

$$\begin{aligned} I = {} & (V + V_{D2} - R_S I)/R_{SH1} + I_{01}\left[e^{\frac{V+V_{D2}-R_S I}{n_1 V_T}} - 1\right] - I_{irr} \\ = {} & \frac{V + \left((-I + I_{02})R_{SH2} - n_2 V_T W\left(\frac{I_{02}R_{SH2}}{n_2 V_T} e^{\frac{(-I+I_{02})R_{SH2}}{n_1 V_T}}\right)\right) - R_S I}{R_{SH1}} \\ & + I_{01}\left[e^{\frac{V + \left[(-I+I_{02})R_{SH2} - n_2 V_T W\left(\frac{I_{02}R_{SH2}}{n_2 V_T} e^{\frac{(-I+I_{02})R_{SH2}}{n_1 V_T}}\right)\right] - R_S I}{n_1 V_T}} - 1\right] - I_{irr} \end{aligned} \tag{8}$$

that can be reorganized as:

$$\begin{aligned} I\left(1 + \frac{(R_S + R_{SH2})}{R_{SH1}}\right) = {} & \frac{V + I_{02}R_{SH2} - n_2 V_T W\left(\frac{I_{02}R_{SH2}}{n_2 V_T} e^{\frac{(-I+I_{02})R_{SH2}}{n_1 V_T}}\right)}{R_{SH1}} - I_{irr} \\ & + I_{01}\left[e^{\frac{V + I_{02}R_{SH2} - (R_S + R_{SH2})I - n_2 V_T W\left(\frac{I_{02}R_{SH2}}{n_2 V_T} e^{\frac{(-I+I_{02})R_{SH2}}{n_2 V_T}}\right)}{n_1 V_T}} - 1\right] \end{aligned} \tag{9}$$

By posing:

$$\Gamma = \left(1 + \frac{(R_S + R_{SH2})}{R_{SH1}}\right) \tag{10}$$

we can obtain the final relation between the current I and voltage V of the two-diode model through just the desired one equation as follows:

$$\begin{aligned} I = {} & \frac{V + I_{02}R_{SH2} - n_2 V_T W\left(\frac{I_{02}R_{SH2}}{n_2 V_T} e^{\frac{(-I+I_{02})R_{SH2}}{n_2 V_T}}\right)}{R_{SH1} + R_{SH2} + R_S} \\ & + \frac{I_{01}}{\Gamma}\left[e^{\frac{V + I_{02}R_{SH2} - (R_S + R_{SH2})I - n_2 V_T W\left(\frac{I_{02}R_{SH2}}{n_2 V_T} e^{\frac{(-I+I_{02})R_{SH2}}{n_2 V_T}}\right)}{n_1 V_T}} - 1\right] - \frac{I_{irr}}{\Gamma} \end{aligned} \tag{11}$$

Although Eq. (11) cannot be posed in an explicit form due to its transcendental nature, it can be easily adopted for several applications or theoretical studies. Moreover it can be directly injected into more complex models without having to use other approaches such as the Modified Nodal Analysis (MNA) method requiring to solve a system of non-linear equations. Lastly, it can be adopted without requiring 'simplifications' or specific assumptions on parameters that, although potentially making the solution procedure easier, can severely limit the accuracy of the fitting routine. In the next section we will discuss the identification problem with all the issues related to its solutions.

3.1. Identification of the two-diode circuit by applying the one-equation model

The Eq. (11) is characterised by 8 parameters (the ones present in the two-diode model, that are $R_{SH1}, R_{SH2}, I_{01}, I_{02}, n_1, n_2, I_{irr}, R_S$) and their identification from experimental measurements is not an easy task. Indeed, it requires the solution of a non-linear least squares problem that can be formulated as

$$\mathrm{MSE} = \frac{1}{N}\sum_{k=1}^{N}\left[I_k^{meas} - I_k^{comp}(V_k^{meas}, X)\right]^2 \tag{12}$$

where N is the number of measurements (I_k^{meas}, V_k^{meas}) available and $I_k^{comp}(V_k^{meas}, X)$ is achieved by exploiting Eq. (11) whereas X is the set of parameters $X = [R_{SH1}, R_{SH2}, I_{01}, I_{02}, n_1, n_2, I_{irr}, R_S]$. Clearly the optimal solution $X_{optimal}$ is the one which minimises the MSE. In this sense it can be solved also in terms of a minimisation problem which uses the above Eq. (12) as a fitness function, as already successfully done for inorganic solar cells/modules (Laudani et al., 2014). The extraction of the 8 parameters from experimental I–V curves is a challenging multimodal problem that could be considered an actual benchmark for any kind of optimisation techniques. Indeed, the presence of several local minima (multimodal problem) prevents using directly deterministic algorithms since they are strongly sensitive to initial guesses: the algorithm could remain trapped in different local minima and thus return different solutions depending on the choice of the initial guesses. With the aim to detect the global optimum (i.e. the best solution), avoiding to wind up into local minima, stochastic algorithms coming from the Artificial Intelligence and Evolutionary Computation can be adopted (Michalewicz and Fogel, 2004). They could be effective in finding the best solution within a multimodal problem, but their convergence times and computational costs are considerably onerous together with, in general, a low degree of accuracy when compared to deterministic algorithms (Fulginei and Salvini, 2007). For this reason, our approach is to use a hybrid optimizer which combines stochastic and deterministic methods. In particular we exploit exploration capability of the Genetic Algorithm (GA) to locate individual candidate solutions, and the strong convergence of the deterministic methods (such as Levemberg–Marquadt) implemented in the *fsolve* Matlab function. The implementation of hybrid optimizer consists of the execution of a fixed number of steps of GA, during which the best solutions are saved on a specific file; at the end of GA, *fsolve* is launched by using the solutions found by GA as initial guess. In this way GA is used for improving the exploration and *fsolve* operates for the refinement of GAs solutions. In addition, in order to be sure to explore all the search space, we ran the hybrid optimizer 10 times achieving a better evaluation of the behaviour of the model together with its results. This is extremely important due to the fact that, as stated before, for such a large search domain there is a strong influence of initial parameter choice on results, which can lead to a premature stop of the fitting procedure due to the presence of local minima.

Table 1
Identification results for naIV100 by using the 8-parameter model on two-diode circuit with $R_S \neq 0$.

Parameter	Sol #1	Sol #2	Sol #3
R_{SH1} (Ω)	1.87187E+03	1.87182E+03	1.87179E+03
R_{SH2} (Ω)	5.43836E+02	5.43820E+02	5.43805E+02
I_{01} (A)	1.36455E−05	1.36375E−05	1.36326E−05
I_{02} (A)	2.30790E−04	2.30775E−04	2.30761E−04
n_1V_T (V)	7.76994E−02	7.76910E−02	7.76859E−02
n_2V_T (V)	4.25934E−02	4.25864E−02	4.25801E−02
I_{irr} (A)	4.35099E−03	4.35100E−03	4.35101E−03
R_S (Ω)	1.43243E−01	1.51266E−01	1.57601E−01
MSE	8.987E−11	8.990E−11	8.992E−11

3.2. Results and discussions

3.2.1. Influence of R_S within the two-diode circuit: from 8-parameter to 7-parameter model

The first interesting result herein discussed regards the influence of the series resistance R_S that seems to be a critical parameter for fitting experimental data. Table 1 shows the three best results related to the measurements data set '"naIV100"', achieved after 10 launches of the above described hybrid optimizer, by supposing $R_S \neq 0$. It is possible to note that whilst the three MSEs are essentially the same, the solutions substantially differ just in the values of R_S. The difference between the largest R_S and the smallest one is around 9%, whereas the others parameters remain practically the same (with differences lower than 0.1%).

We note that R_S and R_{SH2} are strongly correlated and present reverse behaviours in the solutions. Comparing Sol #1 to Sol #3 R_{SH2} decreases whereas R_S increases, however, the sum $R_{SH2} + R_S$ varies by just 0.003%. This indicates that the 8-parameter problem is not well conditioned in terms of the R_S. Indeed, if we do not impose that R_S must be positive, similar results are achieved for negative values of R_S that, obviously, don't have a physical meaning. This can lead to confusion in the physical interpretation of the parameters themselves. Therefore we consider the contribution of R_S as a part of the R_{SH2} and reduce the number of parameters to 7.

3.2.2. Discussion on the results of the 7-parameter model ($R_S = 0$)

As a consequence of the above considerations, we deal with the identification problem by using the same two-diode circuit model

Table 2
Two-diode model identification performed by the 7-parameter model ($R_S = 0$).

Parameter	Not anneal.	a120C5min100	a150C5min100	a180C5min100	a200C5min100
R_{SH1} (Ω)	1.87271E+03	1.28702E+03	1.36971E+03	1.61961E+03	1.45364E+03
R_{SH2} (Ω)	5.44129E+02	2.97303E+02	1.06711E+02	3.52216E+01	4.41601E+01
I_{01} (A)	1.37794E−05	8.37219E−06	3.12466E−05	7.78883E−05	3.40742E−05
I_{02} (A)	2.31048E−04	2.74651E−04	7.84896E−05	1.21165E−04	7.20802E−04
n_1V_T (V)	7.78379E−02	8.66645E−02	1.22951E−01	1.49315E−01	1.23773E−01
n_2V_T (V)	4.27207E−02	3.22771E−02	1.66717E−02	2.93503E−04	2.17601E−02
I_{irr} (A)	4.35082E−03	4.16716E−03	4.39706E−03	5.08416E−03	5.45063E−03
MSE	8.940E−11	2.897E−10	1.345E−09	1.024E−08	9.798E−10

where we assumed $R_S = 0$ (7-parameter model). Now the 10 simulations of GA and *fsolve* all converge to the same solution (i.e. very similar from the numerical and MSE points of views, considering a tolerance of 1E−5 amongst the values of the 10 solutions found for each case). This means that, except in the case of non-convergence, just one run is sufficient to return a meaningful solution from a given *I–V* experimental curve. In particular, it is worth noticing that the achieved MSEs are smaller than the previously ones

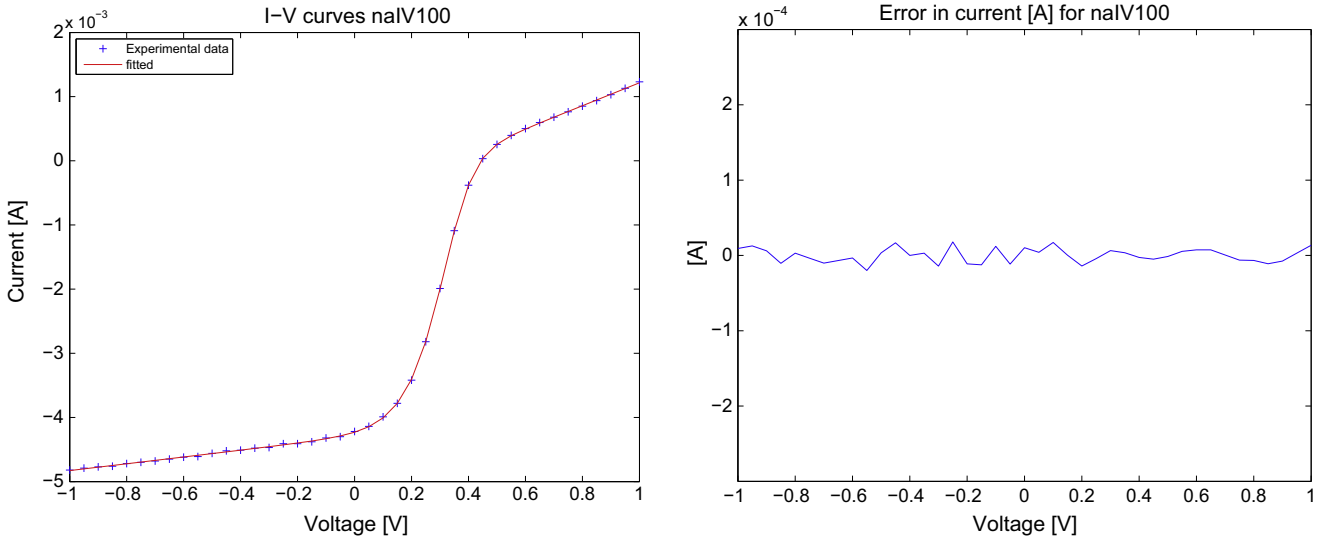

Fig. 3. Experimental and simulated *I–V* curves (left) and absolute error between experimental and simulated curve (right) for the "not annealed" case by using the 7-parameter model.

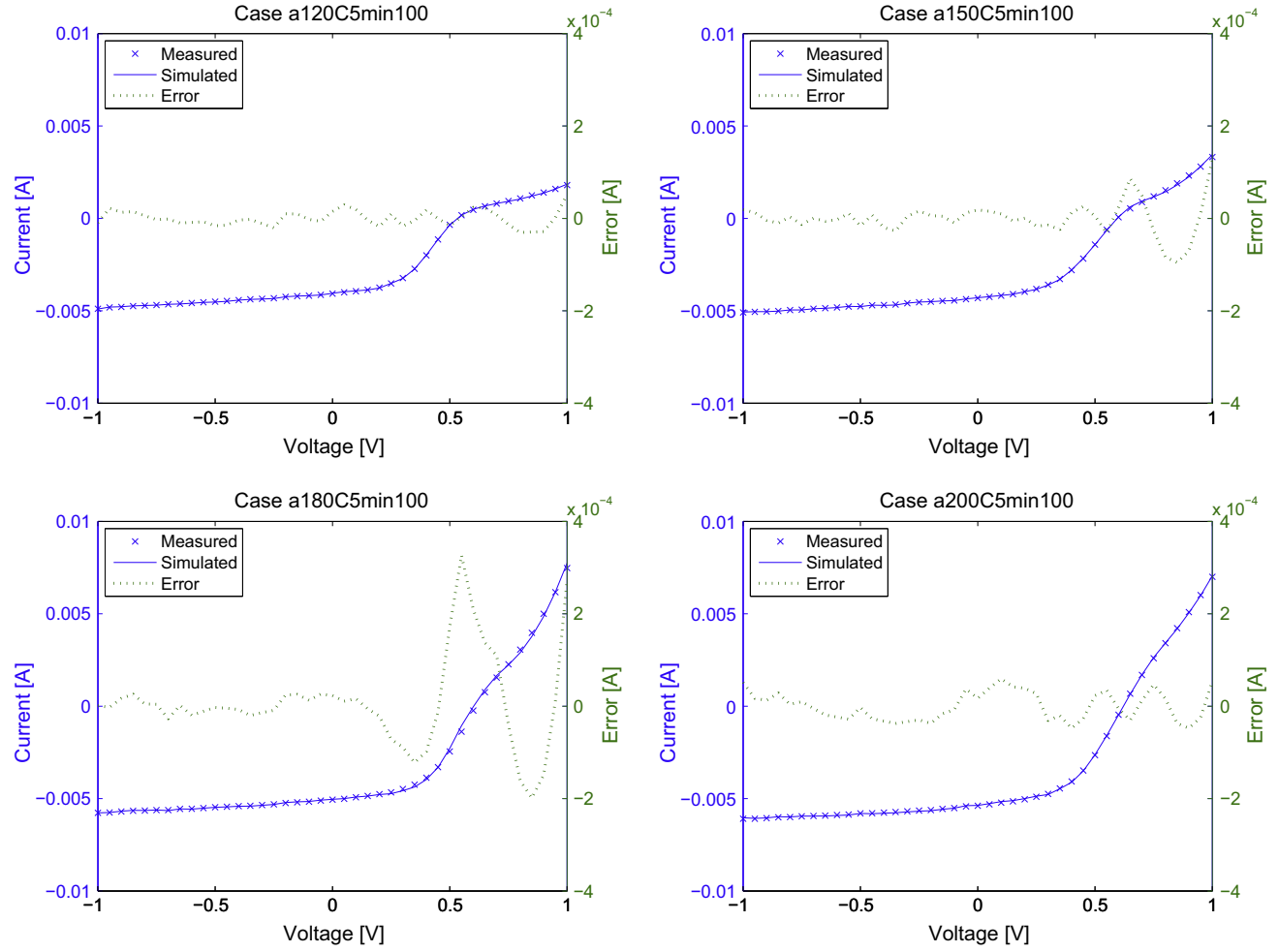

Fig. 4. Absolute error between experimental and simulated curves using the 7-parameter model for "a120C5min", "a150C5min", "a180C5min" and "a200C5min" cases.

obtained with $R_S \neq 0$ (see for example the "not annealed" case in Table 2 where MSE is now equal to 8.94E−11). Fig. 3 shows the I–V curves (experimental and simulated) and the absolute error between experimental and simulated curve for the "not annealed" case. Table 2 reports the results for the "not annealed" case and for the "a150C5min100", "a150C5min100", "a180C5min100" and "a200C5min100" cases. Similar results have been achieved for all the other examined data sets and the related absolute errors on I–V curves are shown in Fig. 4. This confirms that the contribution of R_S seems to be redundant so that it can be removed by considering $R_S = 0$. The resulting 7-parameter model is easier to identify and, above all, seems to be more robust from the modelling point of view (in Appendix A a further comparison between 8-parameter model and 7-parameter model is discussed for the "a120C5min100" dataset). In addition, by using the 7-parameter model, the fitting procedure becomes fast enough (one or two minutes of run times for each I–V curve) to be used also for identifying large datasets.

From the absolute error trends of Fig. 4, it is possible to argue that some problems on identification of the reverse two-diode circuit occur when the current starts to increase again above V_{OC} (after the plateau generated by the s-shape). This is expected as that regime would represent a breakdown (current–voltage curve becomes linear) of the second diode that is not described by the reverse 2-diode model(de Castro et al., 2010). For the considered curves, the more the samples are annealed, the more the increase of current is evident when the voltage is higher than V_{OC}. In the case of annealing at 200 °C the S-shape is removed and the I–V curve looks similar to the one of a single diode (for the same reason in this case the fitting procedure returns low values of MSE). It is also worth noticing that the case at 180 °C, where the s-shape is small but noticeable, is hard to solve and often the hybrid optimizer converges to solutions that are not physically meaningful. Some of the values reported in Table 2 for the solution of the case 180 (achieved after 10 launches of the hybrid optimizer, as said before) seem to be inadequate to describe the problem: indeed the extremely low value of n_2V_T is not acceptable from a physical point of view. In the next paragraph this is overcome by proposing a new three-diode circuital configuration.

4. The generalised 3-diode model one-equation solution

In order to overcome the previously discussed issues and design a generalised circuit capable of describing the full I–V curve, we have tested the effects of the introduction of another diode in the model, placed in anti-parallel with respect of diode D_2 (see Fig. 1(d)). This is a generalisation of the reverse 2-diode model and differs from the one proposed in Fig. 1(c) (Garcia-Sanchez et al., 2013) due to the presence of R_{SH2} and the omission of R_S. The physical concept behind this circuit is that the sub-circuit formed by R_{SH2}, D_2 and D_3 represents an effective series resistance that can be non-linear. The non-linearity that leads to the s-shape in the curves results from a charge injection/extraction process that is voltage dependent and that can have different microscopic origins, as proposed previously (de Castro et al., 2010). The advantage of using a circuit model is that parametrisation of the curves is possible even without detailed knowledge of the complex microscopic processes affecting the device. Below we show that we can also write a one-equation model for this circuit. Let's call V_{D1}, V_{D2} and V_{D3} the direct voltages of the three diodes D_1, D_2 and D_3, respectively, with $V_{D2} = -V_{D3}$. Using Kirchhoff's voltage law we write:

$$V = V_{D1} - V_{D2} = V_{D1} + V_{D3} \tag{13}$$

The voltage V_{D1} can be expressed again as a function of the currents flowing into diode D_1 by using W-Lambert function (see Eq. (2)):

$$V_{D1} = (I + I_{irr} + I_{01})R_{SH1} - n_1V_TW\left(\frac{I_{01}R_{SH1}}{n_1V_T}e^{\frac{(I+I_{irr}+I_{01})R_{SH1}}{n_1V_T}}\right) \tag{14}$$

Obtaining the expression of voltage V_{D2} is a more complex task due to the presence of diode D_3. Nevertheless, it is possible to express the current I as a function of the voltage V_{D2} ($V_{D3} = -V_{D2}$), as follows:

$$I = -V_{D2}/R_{SH2} - I_{02}\left[e^{\frac{V_{D2}}{n_2V_T}} - 1\right] + I_{03}\left[e^{-\frac{V_{D2}}{n_3V_T}} - 1\right] \tag{15}$$

where I_{03} and n_3 are respectively the saturation current and the ideality factor of diode D_3. Now, by considering that $-V_{D2} = V - V_{D1}$ and by using the expression (15), we can write:

$$I = \frac{V - V_{D1}}{R_{SH2}} - I_{02}\left[e^{-\frac{V-V_{D1}}{n_2V_T}} - 1\right] + I_{03}\left[e^{\frac{V-V_{D1}}{n_3V_T}} - 1\right] \tag{16}$$

where the voltage V_{D1} can be substituted by Eq. (14):

$$I = \frac{V - \left[(I + I_{irr} + I_{01})R_{SH1} - n_1V_TW\left(\frac{I_{01}R_{SH1}}{n_1V_T}e^{\frac{(I+I_{irr}+I_{01})R_{SH1}}{n_1V_T}}\right)\right]}{R_{SH2}} - I_{02}\left[e^{\frac{V - \left[(I+I_{irr}+I_{01})R_{SH1} - n_1V_TW\left(\frac{I_{01}R_{SH1}}{n_1V_T}e^{\frac{(I+I_{irr}+I_{01})R_{SH1}}{n_1V_T}}\right)\right]}{n_2V_T}} - 1\right] + I_{03}\left[e^{\frac{V - \left[(I+I_{irr}+I_{01})R_{SH1} - n_1V_TW\left(\frac{I_{01}R_{SH1}}{n_1V_T}e^{\frac{(I+I_{irr}+I_{01})R_{SH1}}{n_1V_T}}\right)\right]}{n_3V_T}} - 1\right] \tag{17}$$

Eq. (17) is the one-equation model for the 9-parameter (i.e. R_{SH1}, R_{SH2}, I_{01}, I_{02}, I_{03}, n_1, n_2, n_3, I_{irr}) model of the three-diode circuit here proposed.

Table 3
Three-diode model identification performed by the 9-parameter model ($R_S = 0$).

Parameter	na	a120	a150	a180	a200
R_{SH1} (Ω)	1.86892E+03	1.27716E+03	1.33442E+03	1.42708E+03	1.43642E+03
R_{SH2} (Ω)	5.60459E+02	3.71525E+02	5.65504E+02	5.48602E+02	4.76586E+01
I_{01} (A)	1.33246E−05	6.59283E−06	2.04833E−05	1.65838E−05	2.93955E−05
I_{02} (A)	2.42450E−04	3.73048E−04	4.42820E−04	6.44319E−04	9.02248E−04
I_{03} (A)	2.17627E−09	4.69249E−06	8.62238E−04	3.37033E−03	8.73843E−07
n_1V_T (V)	7.73731E−02	8.34736E−02	1.12753E−01	1.08020E−01	1.20367E−01
n_2V_T (V)	4.36580E−02	3.85140E−02	3.49134E−02	2.29209E−02	2.77129E−02
n_3V_T (V)	5.58835E−02	1.09726E−01	2.61098E−01	2.72823E−01	4.74311E−02
I_{irr} (A)	4.35109E−03	4.17086E−03	4.40866E−03	5.11985E−03	5.45468E−03
MSE	8.018E−11	1.251E−10	1.364E−10	5.353E−10	7.850E−10

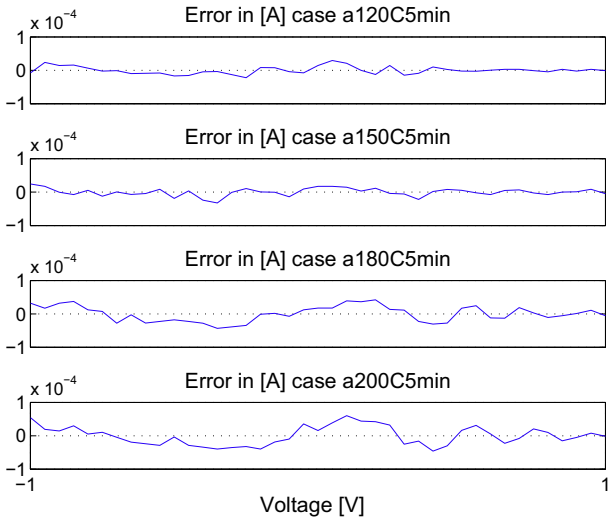

Fig. 5. Error between experimental and simulated curves in the case of 3-diode model for "a120C5min", "a150C5min", "a180C5min" and "a200C5min".

4.1. Discussion on the results obtained by using the proposed 3-diode circuit

As shown for the case of the reverse 2-diode one-equation solution, here we also exploit the synergy between stochastic (GA) and deterministic (Levemberg–Marquadt) methods, in a hybrid optimizer. The possibility to use a one-equation formula facilitates the implementation of the solution procedure and allows us to speed up the analysis and gain insight into the identification problem. The same dataset were used and in Table 3 all the obtained results for the 9-parameter model are summarised. A first interesting result is that the fitting procedure is now more efficient and only a few launches of the optimizer are needed in order to find the optimal solutions. Additionally, if the initial condition are chosen in a reasonable way the convergence is reached quickly (just with a single run of the deterministic optimizer).

In addition, from the modelling point of view it is possible to note that:

(1) the MSE remains extremely low for all the five examined cases and the fitting is very accurate. Also the absolute error on the current is now independent of the voltage, differently from the reverse two-diode case (as shown in Fig. 5).
(2) The naIV100 case does not show an evident increase of current in forward bias after the s-shape kink. Therefore the 3-diode model generates similar parameter values to those of the reverse 2-diode model (except for those parameters related to diode 3 for obvious reasons).
(3) the two more critical cases, "a150C5min" and "a180C5min", now are excellently fitted also in the region where the voltage is higher than V_{OC}.

Therefore the proposed 3-diode model seems to be an optimal generalised circuit model capable of modelling non-ideal current voltage curves as those observed for some organic photovoltaic devices.

5. Conclusions

In this paper, an in-depth analysis of the modelling of organic solar cells with lumped parameter equivalent circuits has been performed by introducing a new single-equation model linking output current with applied voltage. We demonstrated that the proposed single-equation model facilitates the procedure for the extraction of the parameters and allows faster analysis of the identification problem. In particular, we have demonstrated that the contribution of R_S becomes redundant when additional diodes are introduced in the circuit and therefore can be removed. We propose a generalised 3-diode model, where the combination of a resistor and two diodes represents a non-linear series resistance for the photovoltaic equivalent circuit. We show that we can analyse this circuit using a single equation of current as a function of voltage and validate the model by successfully fitting several experimental curves with different degrees of s-shape. We also propose a hybrid optimiser approach that combine genetic algorithms with deterministic methods. This approach allowed very fast and accurate convergence opening the possibility of applying this models to large datasets. We believe such model could be particularly useful for the analysis of degradation in solar cells, where non-ideal current voltage curves often are observed.

Table A.4
Results obtained for "a120C5min100" case by using the 8-parameter model on the 2-diode circuit with $R_S \neq 0$.

Parameter	Sol #1	Sol #2	Sol #3
R_{SH1} (Ω)	1.27789E+03	1.27775E+03	1.27724E+03
R_{SH2} (Ω)	2.93721E+02	2.93663E+02	2.93450E+02
I_{01} (A)	6.63989E−06	6.61477E−06	6.52508E−06
I_{02} (A)	2.71688E−04	2.71641E−04	2.71456E−04
n_1V_T (V)	8.34455E−02	8.33949E−02	8.32127E−02
n_2V_T (V)	2.99484E−02	2.99110E−02	2.97730E−02
I_{irr} (A)	4.17242E−03	4.17251E−03	4.17281E−03
R_S (Ω)	3.19729E+00	3.24875E+00	3.43578E+00
MSE	2.879E−10	2.879E−10	2.879E−10

Conflict of interest

None declared.

Acknowledgments

FAC acknowledges funding from the U.K. Department for Business, Innovation and Skills.

Appendix A. Test of 8-parameter model on a120C5min100

As further example, we report in the Table A.4, three solutions found by using GA and *fsolve* with the 8-parameter model for the experimental data related to the "a120C5min100". Also in this case, the solutions substantially differ for R_S (about 6%) whereas the other parameters are approximately equal to each other and the presence of several different solutions does not exist if we use the 7-parameter model ($R_S = 0$). The only one achieved solution (considering a tolerance of 1E−5 amongst two different solutions) by using the 7-parameter model was previously reported in Table 2.

References

Banwell, T., Jayakumar, A., 2000. Exact analytical solution for current flow through diode with series resistance. Electron. Lett. 36 (4), 291–292.
Castro, F.A., Benmansour, H., Graeff, C.F.O., Nesch, F., Tutis, E., Hany, R., 2006. Nanostructured organic layers via polymer demixing for interface-enhanced photovoltaic cells. Chem. Mater. 18 (23), 5504–5509. http://dx.doi.org/10.1021/cm061660r.
Cheknane, A., Hilal, H.S., Djeffal, F., Benyoucef, B., Charles, J.-P., 2008. An equivalent circuit approach to organic solar cell modelling. Microelectron. J. 39 (10), 1173–1180 <http://www.sciencedirect.com/science/article/pii/S0026269208001134>.
Corless, R.M., Gonnet, G.H., Hare, D.E.G., Jeffrey, D.J., Knuth, D.E., 1996. On the lambert w function. Adv. Comput. Math. 5 (1), 329–359.

de Castro, F., Heier, J., Nuesch, F., Hany, R., 2010. Origin of the kink in current-density versus voltage curves and efficiency enhancement of polymer-c60 heterojunction solar cells. IEEE J. Select. Topics Quant. Electron. 16 (6), 1690–1699.

del Pozo, G., Romero, B., Arredondo, B., 2012. Evolution with annealing of solar cell parameters modeling the s-shape of the current voltage characteristic. Solar Energy Mater. Solar Cells 104 (0), 81–86 <http://www.sciencedirect.com/science/article/pii/S0927024812002243>.

Fulginei, F.R., Salvini, A., 2007. Comparative analysis between modern heuristics and hybrid algorithms. COMPEL – Int. J. Comput. Math. Electr. Electron. Eng. 26 (2), 259–268.

Garcia-Sanchez, F., Lugo-Muoz, D., Muci, J., Ortiz-Conde, A., 2013. Lumped parameter modeling of organic solar cells s-shaped I–V characteristics. IEEE J. Photovolt. 3 (1), 330–335.

Green, M.A., Emery, K., Hishikawa, Y., Warta, W., Dunlop, E.D., 2016. Solar cell efficiency tables (version 47). Prog. Photovolt.: Res. Appl. 24 (1), 3–11. http://dx.doi.org/10.1002/pip.2728 (pIP-15-272).

Heliatek, 2016. Heliatek sets new organic photovoltaic world record efficiency of 13.2% <http://www.heliatek.com/en/press/press-releases/details/heliatek-sets-new-organic-photovoltaic-world-record-efficiency-of-13-2> (retrieved June 10, 2016).

Jain, A., Kapoor, A., 2004. Exact analytical solutions of the parameters of real solar cells using Lambert W function. Solar Energy Mater. Solar Cells 81 (2), 269–277.

Jain, A., Kapoor, A., 2005. A new approach to study organic solar cell using lambert w-function. Solar Energy Mater. Solar Cells 86 (2), 197–205 <http://www.sciencedirect.com/science/article/pii/S0927024804002867>.

Kong, J., Song, S., Yoo, M., Lee, G.Y., Kwon, O., Park, J.K., Back, H., Kim, G., Lee, S.H., Suh, H., 2014. Long-term stable polymer solar cells with significantly reduced burn-in loss. Nature Commun. 5.

Laudani, A., Fulginei, F.R., Salvini, A., 2014. High performing extraction procedure for the one-diode model of a photovoltaic panel from experimental iv curves by using reduced forms. Solar Energy 103 (0), 316–326 <http://www.sciencedirect.com/science/article/pii/S0038092X14000929>.

Mazhari, B., 2006. An improved solar cell circuit model for organic solar cells. Solar Energy Mater. Solar Cells 90 (78), 1021–1033 <http://www.sciencedirect.com/science/article/pii/S0927024805001832>.

Michalewicz, Z., Fogel, D.B., 2004. How to Solve It: Modern Heuristics. Springer, Berlin Heidelberg <http://link.springer.com/10.1007/978-3-662-07807-5>.

Ortiz-Conde, A., Sanchez, F.J.G., Muci, J., 2000. Exact analytical solutions of the forward non-ideal diode equation with series and shunt parasitic resistances. Solid-State Electron. 44 (10), 1861–1864 <http://www.sciencedirect.com/science/article/pii/S0038110100001325>.

Romero, B., del Pozo, G., Arredondo, B., 2012. Exact analytical solution of a two diode circuit model for organic solar cells showing s-shape using lambert w-functions. Solar Energy 86 (10), 3026–3029 <http://www.sciencedirect.com/science/article/pii/S0038092X12002526>.

Romero, B., Pozo, G.D., Destouesse, E., Chambon, S., Arredondo, B., 2014. Circuital modelling of s-shape removal in the current voltage characteristic of TiOx inverted organic solar cells through white-light soaking. Organic Electron. 15 (12), 3546–3551 <http://www.sciencedirect.com/science/article/pii/S1566119914004425X>.

Sandberg, O.J., Nyman, M., Österbacka, R., 2014. Effect of contacts in organic bulk heterojunction solar cells. Phys. Rev. Appl. 1, 024003 <http://link.aps.org/doi/10.1103/PhysRevApplied.1.024003>.

Wagenpfahl, A., Rauh, D., Binder, M., Deibel, C., Dyakonov, V., 2010. S-shaped current–voltage characteristics of organic solar devices. Phys. Rev. B 82 (11), 115306.